Acta Polytechnica CTU Proceedings **56**:1–7, 2026
https://doi.org/10.14311/APP.2026.56.0001

Published by the Czech Technical University in Prague

MODELLING DIAPHRAGM WALLS USING A TIME-DEPENDENT ELASTO-PLASTIC MATERIAL MODEL

Daniela Marková*, Juraj Chalmovský

Brno University of Technology, Faculty of Civil Engineering, Institute of Geotechnics, Veveří 331/95, 602 00 Brno, Czech Republic

* corresponding author: Daniela.Markova@vutbr.cz

Abstract. This paper utilizes an advanced time-dependent elastoplastic material model for the modelling of diaphragm walls via the Finite Element Method (FEM). After describing the time-dependent behaviour of concrete, the Shotcrete material model is specified, and calibration of the material model in long-term conditions based on laboratory testing is carried out. Finally, a real boundary value problem of deep excavation supported by permanent diaphragm walls with the strut is solved. Various strategies of modelling are used and compared. The Shotcrete material model allows simulating creep deformations continuously (that is not stepwise), but when limiting tensile and compressive strength, it is necessary to include reinforcement.

Keywords: Diaphragm wall, creep, shrinkage, material model, biaxial test, calibration, finite element method, Plaxis 2D.

1. Introduction

This paper analyses the impact of time-dependent phenomena in concrete on the long-term performance of diaphragm walls. In this type of construction, an elasticity modulus and strength develop over time, as well as creep and shrinkage deformations, which then tend to influence the diaphragm wall performance throughout the construction lifetime. Linear elastic material models are usually used for the material of the diaphragm walls themselves. This engineering approach neglects the influence of time-dependent behaviour, which can significantly impact deformations and stresses in construction. An approach closer to reality is based on modelling a concrete structure by combining a volumetric and plate element. By deactivating a plate element in long-term conditions, the creep effect on the long-term stiffness is simulated. The major drawback of this approach is a stepwise change of stiffness.

None of the above-mentioned approaches provide a complex analysis as time goes on. The application of an advanced constitutive model for concrete [1, 2] offers the advantage of including continuous time-dependent behaviour in concrete as well as evaluating deformations and internal forces at every moment throughout the structure's lifetime.

2. Time-dependent behaviour of concrete

Rules of concrete construction design are described in Eurocode 2 [3], where different types of concrete, based on compressive strength, are defined. The compressive strength of concrete is evaluated for time after 28 days, as well as the Young's elastic modulus and the tensile strength specified for the concrete class. Through concrete curing, these characteristics increase and simultaneously influence the final shape of construction and an internal forces redistribution, especially in monolithic structures.

2.1. Increase in elasticity modulus and strength characteristics of concrete

According to Eurocode 2 [3], concrete cures during the first 28 days and within this time, a compression and tensile strength and elasticity modulus increase up to the final value corresponding to the concrete class. The characteristics values calculation in time is based on a cement type (R, N, S). Cement type R ensures rapid characteristics increase from the beginning of curing, cement type N increases more slowly, and cement type S increases characteristics very slowly. For concrete class C20/25 are curves of strength and modulus increase shown in Figure 1, Figure 2 and Figure 3. Whereas the compressive strength and elasticity modulus rise to a value corresponding to the concrete class till 28 days, the tensile strength evolves even after this time.

2.2. Creep of concrete

Creep, unlike shrinkage, is a load-dependent process (Figure 4a). It depends mainly on the following factors: a) load value, b) load duration, and c) concrete age at the moment of load application. According to Eurocode 2 [3], the creep strain depends on the value of the creep coefficient $\varphi(\infty, t_0)$. This coefficient can be calculated using the recommended procedure [3], and input values are the ambient humidity, size of the structure and the concrete composition. It is necessary to draw attention to the fact that Eurocode 2 [3] considers creep only in compression, and the effect of creep

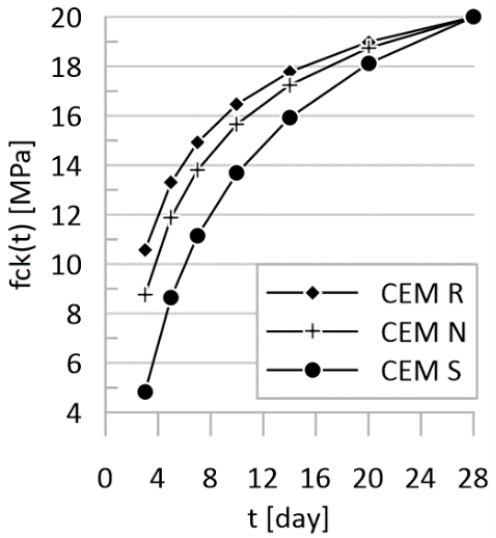

Figure 1. Increase in compressive strength.

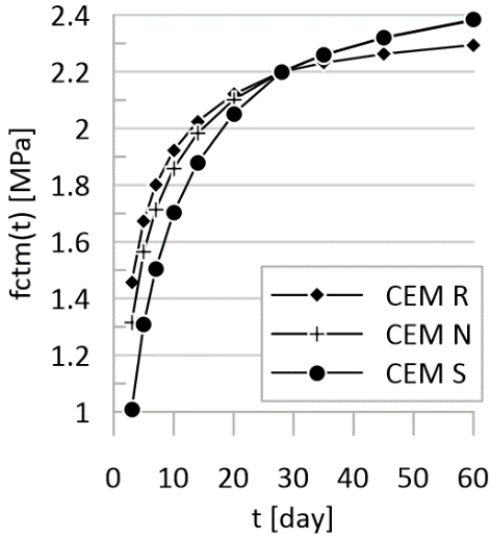

Figure 2. Increase in tensile strength.

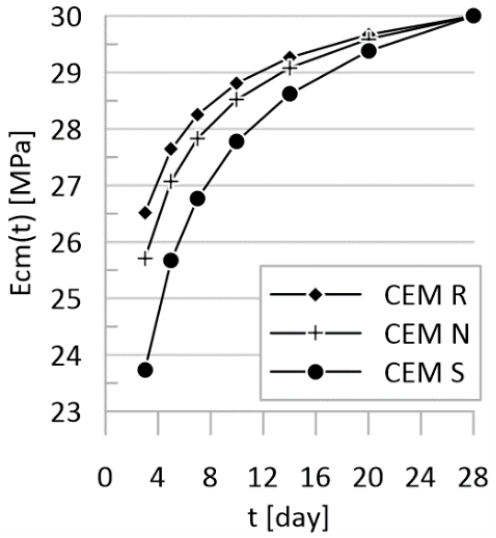

Figure 3. Increase in elasticity modulus.

in tension cannot be evaluated using this standard. This limitation could cause problems while calculating creep strains for elements subjected to bending, where compressed and tension fibres are on the opposite surface. Another restriction of Eurocode 2 [3] occurs when the load value changes during the construction lifetime. A creep strain value can be calculated only by depending on the current load value. The history of stress changes in a structure, leading to permanent shape changes, cannot be considered.

2.3. Shrinkage of concrete

Shrinkage occurs throughout the whole construction lifetime, regardless of the load value. The progress of element shrinkage depends on the ambient humidity and the concrete composition (illustration of this phenomenon is in Figure 4b). According to Eurocode 2, shrinkage strain is divided into two parts: drying shrinkage strain (ongoing throughout the construction lifetime) and autogenous shrinkage strain (linear function of concrete compressive strength, in major part it develops in the first few days of concrete curing). Eurocode 2 determines a procedure leading to the final shrinkage strain evaluation. The governing variables of this calculation process are ambient humidity, concrete strength class and thickness of an element.

3. Advanced material model – shotcrete material model

The utilized material model Shotcrete (further noted as SH) was initially developed for the modelling of primary tunnel linings using the New Austrian Tunnelling Method (NATM). This material model can be used in various applications where it is necessary to include the influence of the time-dependent behaviour of concrete. The current engineering approach of time-dependent analysis consists of step changes of the elasticity modulus in the calculation phases, and it is not able to realistically consider gradual changes in concrete and their influence on the construction behaviour. This elastoplastic SH model includes strain hardening and softening as well as time-dependent behaviour, such as a) time-dependent strength and stiffness, b) ductility, c) creep, and d) shrinkage. The following paper is focused on the latter two factors.

3.1. Material model definition

Two failure surfaces are implemented in the SH model: Mohr-Coulomb (in compression) and Rankine [5] (in tension).

Hardening and softening rules are based on [1] and are different for compression and tension. The hardening-softening diagram in compression is shown in Figure 5a. On the horizontal axis is the hardening-softening parameter in compression $H_c = \varepsilon_3^p/\varepsilon_{cp}^p$, where ε_{cp}^p is the strain at which the compressive strength is reached, and ε_3^p is the current value of the minor plastic strain. On the vertical axis is the

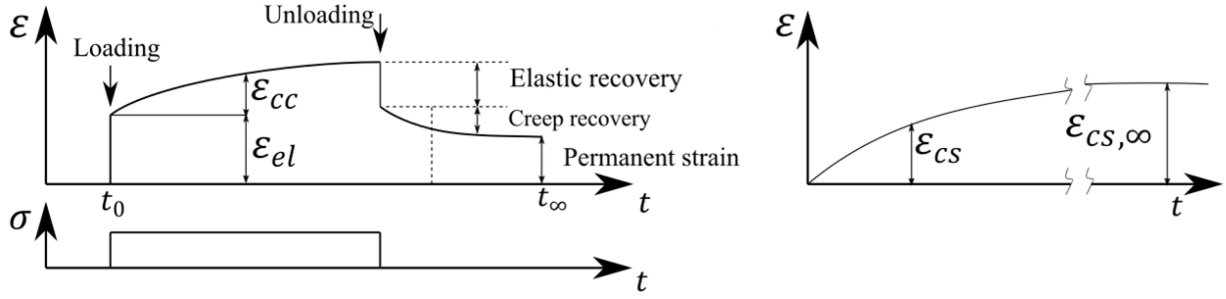

(A). Creep. (B). Shrinkage.

FIGURE 4. Illustration of time-dependent phenomena in concrete (taken from [4] and adjusted).

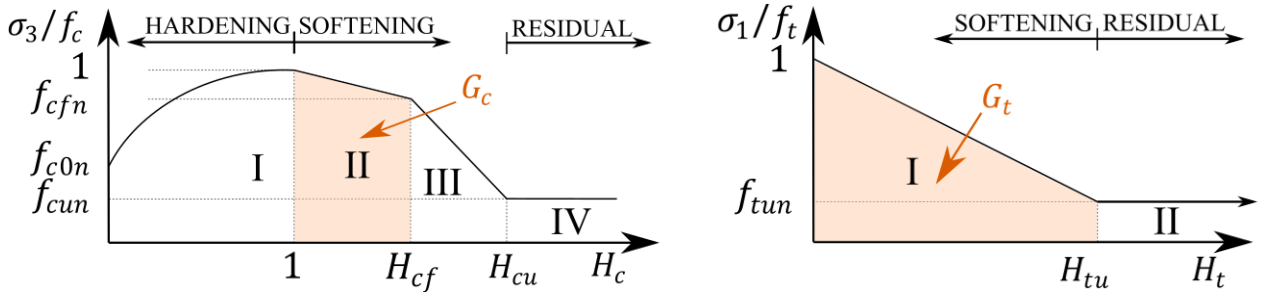

(A). Compression. (B). Tension.

FIGURE 5. Graphical illustration of SH model hardening-softening behaviour (taken from [1] and adjusted).

ratio of the current minor stress and compressive strength σ_3/f_c . The diagram consists of four parts: I) nonlinear hardening, II) linear softening, III) linear softening, and IV) residual strength. If σ_3 is lower than f_{c0n}, only elastic strains occur. The area under the second part of a curve is fracture energy in compression G_c.

The softening in tension is shown in Figure 5b. On the horizontal axis is the hardening-softening parameter in tension $H_c = \varepsilon_1^p/\varepsilon_{tu}^p$, where ε_{tu}^p is a plastic strain, when tensile strength is reached, and ε_1^p is the current value of major plastic strain. On the vertical axis is the ratio of major stress and tensile strength σ_1/f_t . The diagram consists of two parts: I) linear softening, and II) residual strength. The area under the first part of a curve is fracture energy in tension G_t.

3.2. TIME-DEPENDENT BEHAVIOUR OF CONCRETE

As mentioned above, the SH model is able to simulate the time-dependent behaviour of concrete.

Total strains are calculated as the sum of four components: elastic, plastic, creep, and shrinkage according to Formula (1).

$$\varepsilon = \varepsilon^{el} + \varepsilon^{pl} + \varepsilon^{cr} + \varepsilon^{shr} \tag{1}$$

The increase in Young's elasticity modulus during concrete curing is defined according to Formula (2) where E_1 and E_{28} are the concrete elasticity modulus (in kPa) after 1 day and 28 days of curing, respectively. Parameter s_{stiff} (dimensionless) governs the rate of increase in elasticity modulus and can be calculated using Formula (3).

Young's elasticity modulus $E(t)$ (in kPa) at a given the time t (in days), can be calculated using Formula (2). The elasticity modulus value after 28 days corresponds to the concrete strength class, and the recommended value of the ratio E_1/E_{28} is between 0.5 and 0.7.

$$E(t) = E_{28} \cdot e^{s_{stiff}(1-\sqrt{28/t})} \tag{2}$$

$$s_{stiff} = \frac{-\ln(E_1/E_{28})}{\sqrt{28}-1} \tag{3}$$

The increase in strength during concrete curing is defined according to Formula (4) where $f_{c,1}$ and $f_{c,28}$ are the concrete compressive strength (in kPa) after 1 day and 28 days of curing, respectively. Parameter $s_{strength}$ (dimensionless) governs the rate of increase in compressive strength and can be calculated using Formula (5).

Compressive strength $f_c(t)$ (in kPa) at a given the time t (in days), can be calculated using Formula (4). The compressive strength value after 28 days corresponds to the concrete strength class, and the recommended value of the ratio $f_{c,1}/f_{c,28}$ is between 0.2 and 0.3.

$$f_c(t) = f_{c,28} \cdot e^{s_{strength}(1-\sqrt{28/t})} \tag{4}$$

$$s_{strength} = \frac{-\ln(f_{c,1}/f_{c,28})}{\sqrt{28}-1} \tag{5}$$

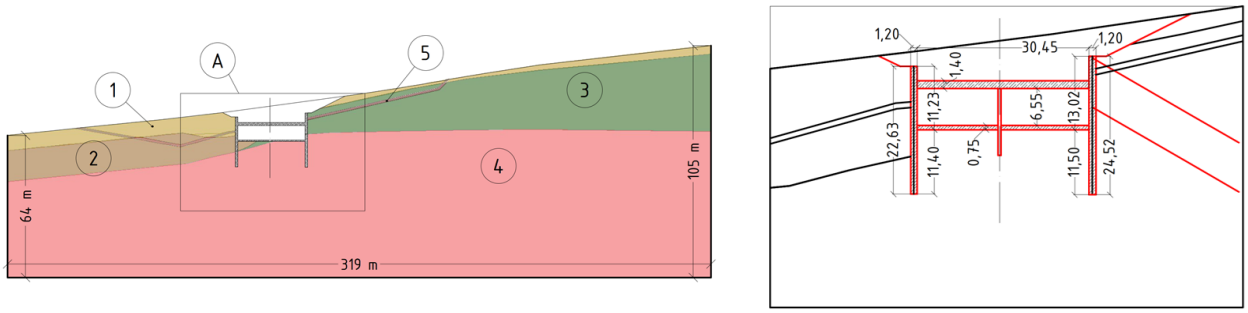

(A). Geological conditions.

(B). Geometry of boundary value problem.

Figure 6. Graphical illustration of real boundary value problem.

A young concrete shows ductile behaviour with a high value of plastic strain before reaching the compressive strength, which later rapidly decreases. In the used material model, plastic ductility is characterized by the parameter ε^p_{cp}. Three input values of this parameter at different time intervals – 1 hour $\varepsilon^p_{cp,1h}$, 8 hours $\varepsilon^p_{cp,8h}$ and 24 hours $\varepsilon^p_{cp,24h}$ – are considered.

Creep is defined by a viscoelastic element. The additional creep strain, $\varepsilon^{cr}(t)$ (dimensionless), at a given time t (in days) is defined according to Formula (6) where σ is the actual stress state (generally a second-order tensor, here using Voigt formula it is a vector, in kPa), D is the stiffness matrix (generally a fourth-order tensor, here it is a second-order tensor, in kPa), and t_0 (in days) marks the beginning of the load application. The value of the creep strain is directly managed by two creep parameters φ^{cr} (ratio between creep and elastic deformation, dimensionless), and t^{cr}_{50} (time in days required to achieve 50 % creep strain). It is recommended to set the value of the creep factor in accordance with the standards [3, 6, 7], and the value of parameter t^{cr}_{50} is recommended to be chosen within the range of 1 to 5 days [8].

$$\varepsilon^{cr}(t) = \frac{\varphi^{cr}\sigma}{D} \cdot \frac{t - t_0}{t + t^{cr}_{50}} \tag{6}$$

The definition of shrinkage in the used material model is similar to the definition of creep. There are two basic input parameters $\varepsilon^{shr}_{\infty}$ (final shrinkage strain, dimensionless) and t^{shr}_{50} (time in days needed to achieve 50 % of shrinkage strain). The actual shrinkage strain $\varepsilon^{shr}(t)$ (dimensionless) can be calculated using Formula (7). Shrinkage, unlike creep, does not depend on the value of stress and the input variables in Formula (7) are shrinkage parameters $\varepsilon^{shr}_{\infty}$ and t^{shr}_{50}. Recommended values for $\varepsilon^{shr}_{\infty}$ range from -0.0002 to -0.0006, while for t^{shr}_{50} range from 28 to 100 days [8].

$$\varepsilon^{shr}(t) = \varepsilon^{shr}_{\infty} \cdot \frac{t}{t + t^{shr}_{50}} \tag{7}$$

4. Real boundary value problem

In the following chapter, a boundary value problem of deep excavation supported by diaphragm walls and struts in 2 levels is solved to compare different approaches to evaluate the influence of the creep of concrete.

4.1. Geological conditions

Geological conditions are shown in Figure 6a. Geotechnical conditions are influenced by the presumed existence of a slip surface. Under the Quaternary sediments (in Figure 6a no. 1), underlying silty clays of the Pliocene age (in Figure 6a no. 2) and clays to silty clays of the Miocene age (in Figure 6a no. 3) are present. The Miocene-age clays are interbedded with thin sandy layers. The deeper layers of the Neogene sediments are represented by claystone of the Paleogene age (in Figure 6a no. 4) in the different stages of weathering. The presumed slip surface is considered as a 1 m thick polygonal layer, for which critical strength parameters are used. The subsoil is modelled with the material model Hardening soil with small strain stiffness [9], and for rocks, the Mohr-Coulomb material model is used.

4.2. Geometry, material model, building phases, input parameters

The excavation is supported by two monolithic diaphragm walls with a thickness of 1 200 mm, combined with struts in two levels (in Figure 6b). The upper strut is non-continuous, with a width of 1 200 mm and height of 1 400 mm with an axial distance of 6.6 m. The bottom strut is located under road construction and is continuous, with a thickness of 750 mm. The excavation width is 31.8 m. The left and right diaphragm wall are 22 m and 25 m long, respectively. Diaphragm walls and struts are made from reinforced concrete of concrete class C30/37 with a density of 25 kN m^{-3}.

All the SH model input parameters are summarised in Table 1. Creep and shrinkage parameters were calibrated by the authors based on laboratory tests [10]. Details of this calibration were previously described in [11] and [12], and the material characteristics of soil and rock are desribed in [11].

The finite element model was 319 m long and 105 m high to eliminate the influence of boundary conditions. Construction stages were treated as consoli-

Param.	E_{28} [kN m^{-2}]	ν [–]	$f_{c,28}$ [kN m^{-2}]	f_{c0n} [–]	f_{cfn} [–]	f_{cun} [–]	$G_{c,28}$ [kN m^{-1}]
Value	$33{\cdot}10^6$	0.15	$30{\cdot}10^3$	0.2	0.1	0.1	70
Param.	φ_{max} [°]	ψ [°]	γ_{fc} [–]	$f_{t,28}$ [kPa]	f_{tun} [–]	$G_{t,28}$ [kN m^{-1}]	γ_{ft} [–]
Value	40	5	1	$3{\cdot}10^3$	$1{\cdot}10^{-3}$	0.148	1
Param.	t_{hydr} [day]	E_1/E_{28} [–]	$f_{c,1}/f_{c,28}$ [–]	${\varepsilon_{cp,1h}}^p$ [–]	${\varepsilon_{cp,8h}}^p$ [–]	${\varepsilon_{cp,24h}}^p$ [–]	a [–]
Value	28	0.65	0.3	-0.03	$-1 \cdot 10^{-3}$	$-0,7 \cdot 10^{-3}$	20
Param.	${\varepsilon_\infty}^{shr}$ [–]	${t_{50}}^{shr}$ [day]	φ^{cr} [–]	${t_{50}}^{cr}$ [den]			
Value	$-2 \cdot 10^{-5}$	86	0.8	40			

TABLE 1. Summary of SH model material parameters used in the boundary value problem.

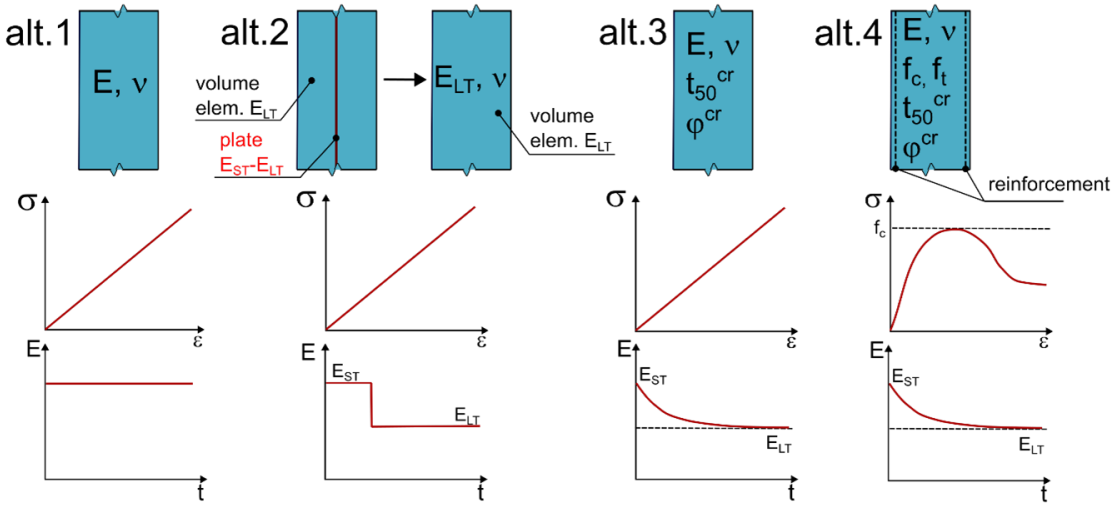

FIGURE 7. Illustration of calculation alternatives (from left side: alt. 1, alt. 2, alt. 3 and alt.4).

dation analyses: apart from primary consolidation of low-permeable Neogene subsoils, time-dependent creep and shrinkage strains occur in concrete structures. The total simulated construction time was 150 days, followed by the rest of the structure lifetime (30 years).

4.3. CALCULATION VARIANTS

Four modelling strategies were used (Figure 7), which differ only by a material model (volumetric and plate elements) used for concrete elements (diaphragm walls and struts). Geometry and geological conditions were the same in all alternatives.

The most common strategy is to model the diaphragm wall using the linear elastic material model and to neglect time-dependent concrete behaviour (alt. 1).

In the second approach (alt. 2), the diaphragm wall is modelled by two element types: volumetric and plate element. Together, they have full short-term stiffness (E_{ST}). The creep effect is simulated by the plate element deactivation, while the volumetric elements with long-term stiffness (E_{LT}) remain active. In terms of the stress-strain behaviour – a linear elastic material model is assigned to both elements. In this way, it is possible to simulate stiffness decrease, but only stepwise, without a continuous decrease in time.

The third approach (alt. 3) considers a full-time-dependent approach, using the SH model for both diaphragm walls and struts. All concrete structures are modelled using volume elements. The limited tensile strength of concrete is not considered (artificially high strengths are used in the SH model).

As in the third alternative, so in the fourth strategy (alt. 4), the full time-dependent approach with continuous development of creep and shrinkage strains is involved. Furthermore, realistic stress-strain behaviour with limited tensile and compressive strength is also considered. This solution requires addition of reinforcement which will transfer tensile stresses in regions where the tensile strength was reached. This was done by using of plate elements on the outer and inner surface of the diaphragm wall.

This alternative should be the most accurate to the actual construction behaviour from the considered alternatives. A disadvantage of this modelling method is (compared to the previous approach) that it involves a more complicated process of obtaining internal forces from the mathematical model. The axial forces in reinforcement need to be multiplied by the distance to the wall midpoint and combined with bending moments reached from the volume element.

4.4. COMPARISON RESULTS FOR CALCULATION VARIANTS

Horizontal displacement and bending moments for all modelling alternatives are shown for the right di-

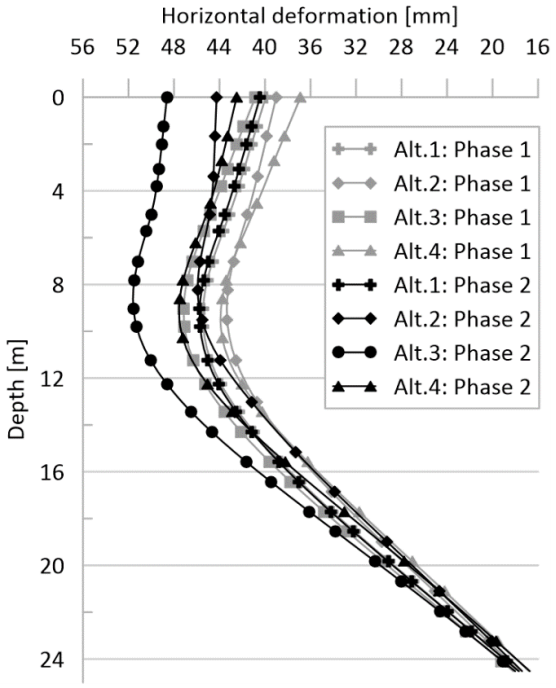

Figure 8. Horizontal deformations of right diaphragm wall – alternatives comparison.

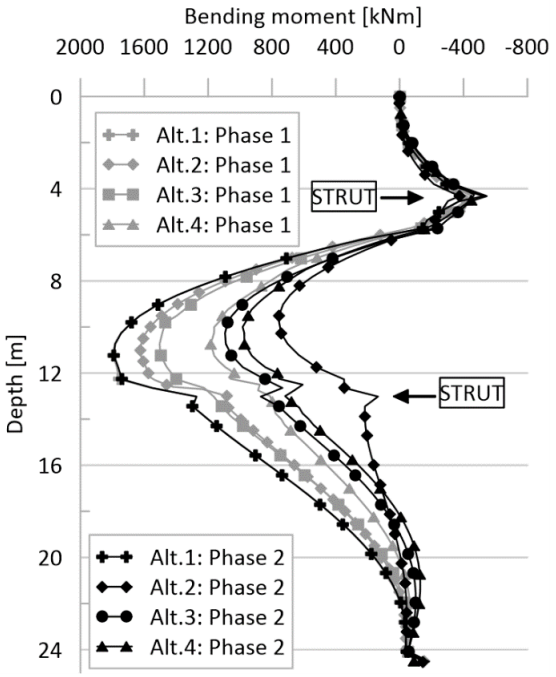

Figure 9. Bending moments in right diaphragm wall – alternatives comparison.

aphragm wall in Figures 8 and 9, respectively. Results for two construction stages are plotted: Phase 1 = Finished construction, Phase 2 = End of construction lifetime (30 years).

Apart from the first modelling alternative, horizontal displacements increase and bending moments decrease from the first case to the second case. These changes are caused solely by additional creep and shrinkage strains of struts and diaphragm walls as results from the two analysed phases are identical in alt. 1. In this alternative, the highest bending moments and the lowest horizontal displacements in the second phase were obtained from all alternatives because high initial (short-term) stiffness is preserved during the whole calculation.

Computed maximum horizontal displacements and displacements at the top of the right diaphragm wall throughout the construction lifetime are shown for the fourth alternative in the logarithmic scale (Figure 10). Similarly maximal bending moments are plotted in Figure 11. Creep and shrinkage phenomena led to a 15,2 % (top) an 8,3 % (max.) increase in horizontal deformations and 17,0 % decrease in max. bending moments at the end of a lifetime compared to the end of construction.

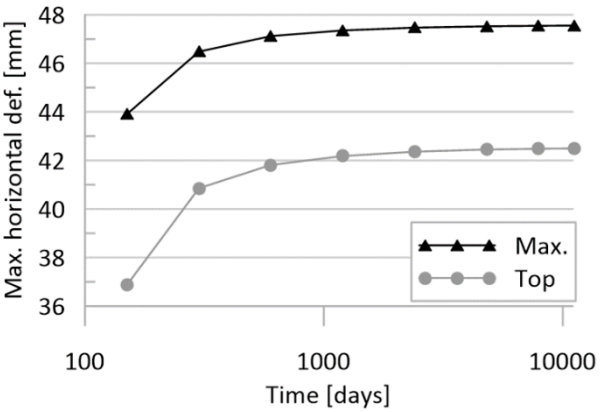

Figure 10. Horizontal deformation progression in time – alt. 4.

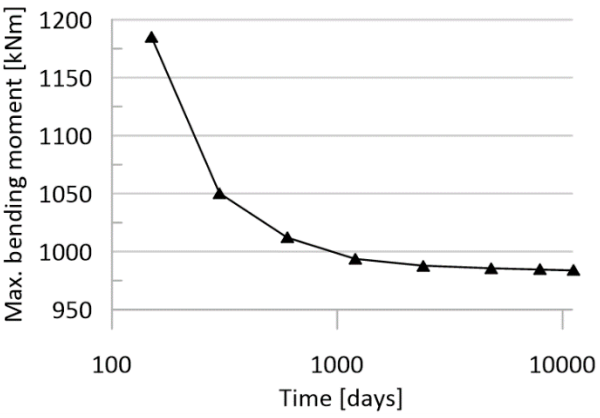

Figure 11. Maximal bending moment progression in time – alt. 4.

5. Conclusions

Three modelling strategies of concrete structural elements capable of simulating creep effects were analysed in this study. The simplest one is based on a combination of volumetric and plate elements in short-term conditions with the subsequent deactivation of the plate element in short-term conditions.

Although simple, continuous increase of creep strains over a long time period is not considered.

The complex approach, based on a combination of an advanced time-dependent elastoplastic material model for concrete and a pair of plate elements representing longitudinal steel reinforcement, offers the possibility of construction analysis at every moment of the construction lifespan. For this approach, the appropriate material model parameter choice is crucial. After performing a material model calibration in laboratory tests, the boundary value problem of a deep cut supported by permanent cast in-situ diaphragm walls was analysed. The calculation results show no negligible influence of time-dependent behaviour throughout the construction lifetime (30 years) since the maximal bending moment decreases by 19,1 %, and the horizontal deformation increases from 8,3 % to 15,2 %.

Acknowledgements

This paper was undertaken within a PhD study in the Faculty of Civil Engineering, BUT.

References

[1] R. Schütz, D. M. Potts, L. Zdravkovic. Advanced constitutive modelling of shotcrete: Model formulation and calibration. *Computers and Geotechnics* **38**(6):834–845, 2011. https://doi.org/10.1016/j.compgeo.2011.05.006

[2] B. Schädlich, H. F. Schweiger. A new constitutive model for shotcrete. In *Numerical Methods in Geotechnical Engineering*, pp. 103–108. Computational Geotechnics Group. Institute for Soil Mechanics and Foundation Engineering, Graz University of Technology, Austria, 2014.

[3] EN 1992-1-1: 2004+A1:2014. Eurocode 2: Design of concrete structures – General rules and rules for buildings. European Committee for Standardization, Brussels, 2014.

[4] J. G. MacGregor. *Reinforced Concrete : Mechanics and design*. Third Edition. Prentice-Hall, Inc., New Jersey, 1997. ISBN 0-13-233974-9.

[5] W. J. M. Rankine. On the stability of loose earth. *Philosophical Transactions of the Royal Society of London* (147):9–27, 1857. https://doi.org/10.1098/rstl.1857.0003

[6] *CEB-FIP model code. Design code – comite Euronational du Beton*. Thomas Telford, London, 1990.

[7] EN 14487-1:2022. Sprayed concrete – Part 1: Definitions, specifications and conformity. European Committee for Standardization, Brussels, 2022.

[8] *PLAXIS Materials Model Manual 2019: Plaxis bv*. Bentley Systems, Incorporated, 2019. ISBN 978-90-76016-27-6.

[9] T. Benz. *Small strain stiffness of soils and its numerical consequences*. Institut für Geotechnik, Universität Stuttgart, Stuttgart, 2007. ISBN 978-3-921837-55-9.

[10] N. Ranaivomanana, S. Multon, A. Turatsinze. Basic creep of concrete under compression, tension and bending. *Construction and Building Materials* **38**:173–180, 2013. 25th Anniversary Session for ACI 228 – Building on the Past for the Future of NDT of Concrete. https://doi.org/10.1016/j.conbuildmat.2012.08.024

[11] D. Šindelářová. *Modelování podzemních stěn pomocí časově závislého elasto-plastického materiálového modelu [In Czech; Modelling of diaphragm walls using time-dependent elasto-plastic material model]*. Master's thesis, Brno University of Technology, Faculty of Civil Engineering, Brno, 2022. [2025-11-15]. https://www.vut.cz/www_base/zav_prace_soubor_verejne.php?file_id=235377

[12] D. Šindelářová, J. Chalmovský. Numerical analysis of creep and shrinkage behaviour of concrete during laboratory tests using advanced constitutive model. In *Juniorstav 2024: Proceedings 26th International Scientific Conference Of Civil Engineering*, pp. 1–10. Vysoké učení technické v Brně, Fakulta stavební, 2024. https://doi.org/10.13164/juniorstav.2024.24065